Mechanical Characterization of Closed-Cell Polyolefin Foams

M. A. RODRÍGUEZ-PÉREZ,[1] J. I. VELASCO,[2] D. ARENCÓN,[2] O. ALMANZA,[3] J. A. DE SAJA[1]

[1] Departamento de Física de la Materia Condensada, Cristalografía y Mineralogía, Facultad de Ciencias, Prado de la Magdalena s/n, Universidad de Valladolid 47011, Valladolid, Spain

[2] Department de Ciència dels Materials y Enginyeria Metal-lúrgica, Escola Técnica Superior d'Enginyers Industrials de Barcelona, Avda. Diagonal, 647, 08028, Barcelona

[3] Departamento de Física, Universidad Nacional de Colombia, Santafé de Bogota, Colombia

Received 7 August 1998; accepted 22 June 1999

ABSTRACT: Three different experimental techniques [compression experiments at low strain rates, instrumented falling-weight impact tests, and dynamic mechanical analysis (DMA)] have been used for the mechanical characterization of a collection of crosslinked closed-cell polyolefin foams of different chemical compositions, densities, and type of cellular structure. The experimental results that it is possible to obtain from each technique are shown, and related to the different applications of these materials. The relationships between the structure and the mechanical properties are also presented. © 2000 John Wiley & Sons, Inc. J Appl Polym Sci 75: 156–166, 2000

Key words: mechanical properties of foams; polyolefin foams; falling-weight impact tests; dynamic mechanical analysis

INTRODUCTION

A variety of properties, such as light weight, chemical resistance and inertness, buoyancy, good aging, cushioning performance, thermal and acoustic insulation, and recyclabibility have helped polyolefin foams penetrate the automotive, packaging, building and construction, marine, medical, and sports and leisure markets.

With advances in technology, foamed polyolefins are becoming more efficient and adaptable to specific mechanical needs. The investigation on the mechanical response of these materials is essential to select the most representative one for each application. Due to this reason, in this work, we have studied the mechanical response of a collection of closed cell polyolefin foams using three different techniques that are related to different applications of these materials. These techniques are: compression experiments at low strain rates, dynamic mechanical analysis (DMA), and instrumented falling-weight impact tests.

Because most applications of foams cause them to be loaded in compression (packaging, thermal insulation in floors, core of sandwich panels, etc.), compression experiments at low strain rates are the most usual way to characterize the mechanical properties of foams,[1] but on the other hand, it is clear that more experimental techniques are necessary to obtain the mechanical response of these materials to other kind of inputs as, for example, vibrations and impacts.

The response to low-frequency vibrations and the energy dissipation capabilities of foams can be studied by means of dynamic mechanical analysis (DMA), which has long been employed in the

Correspondence to: M. A. Rodríguez-Pérez.

Journal of Applied Polymer Science, Vol. 75, 156–166 (2000)
 CCC 0021-8995/00/010156-11

Table I Basic Characteristics of the Foams under Study

Sample	Kind of Foaming Process	Chemical Composition	Density (kg/m^3)	Thickness (mm)
NLB1106	Alveolen	50% LDPE, 50% LLDPE	89	5.83
NLB1408	Alveolen	50% LDPE, 50% LLDPE	67	7.80
NLB2910	Alveolen	50% LDPE, 50% LLDPE	33	10.00
NA1106	Alveolen	100% LDPE	85	6.31
NA2006	Alveolen	100% LDPE	48	6.23
NA3308	Alveolen	100% LDPE	29	7.92
NEE1109	Alveolen	90% EVA, 10% LDPE	86	8.71
NSR2512	Alveolen	50% EPR, 50% EVA	36	12.06
NT0905	Alveolen	60% LDPE, 40% HDPE	105	4.73
NT2510	Alveolen	60% LDPE, 40% HDPE	37	10.81
TL2005	Alveolit	50% LDPE, 50% LLDPE	49	5.09
TL3008	Alveolit	50% LDPE, 50% LLDPE	31	8.43
TA1504	Alveolit	100% LDPE	62	4.02

study of the viscoelastic response of polymers. Dynamic mechanical properties are very important in applications such as cushioning and damping systems[2] (constrained layer system, extensional layer system). Moreover, the fact that DMA can be used to follow main chain and side groups motions in polymers makes it a powerful technique for the characterization of polymer structures, and in particular, of complex porous materials.

The response of foams to impacts is a very important subject that has not been widely studied. Polyolefin foams are viscoelastic materials, and due to this reason their mechanical properties are strain rate dependent. Furthermore, the response to impacts is related with a very important application such as packaging. In this sense, some previous works[3,4] have applied falling-weight techniques to characterize thermoplastic foams using a plane compression headstock and an accelerometer joint to the falling mass. This test configuration does not take into account that the impact is often caused by a sharp element. We think that the use of a narrow hemispherical headstock in instrumented falling-weight impact tests permits simulation of the collision of the foam with a relatively sharp element at high speed, as could happen in any packaging application.

On the other hand, there are some detailed studies on the influence of the foam density on the mechanical properties of semicrystalline foams, but there are not detailed studies about the influence of the morphology of the base polymer on the final properties of the foams. The main reason for the lack of progress in the comprehension of the mechanical properties of semicrystalline foams is crystallinity and complications introduced by the resulting structure and morphology. In this work, foams made of different types of polyethylene have been characterized, and their mechanical properties compared to determine the influence of the morphology of the base polymer on the final properties of the foams.

Bearing these ideas in mind, the aims of this work are first, to present the mechanical properties of a collection of polyolefin foams obtained from different experimental techniques, and second, to study the relationships between the structure, chemical composition, and density of the foams with their mechanical properties.

MATERIALS

The acronym, density, thickness and chemical composition of the industrial samples under study are summarized in Table I. These foamed samples are made from LDPE (low-density polyethylene), i.e., TA and NA foams; blends of LDPE and HDPE (high-density polyethylene), i.e., NT foams; blends of LDPE and LLDPE (linear low-density polyethylene), i.e., NLB and TL foams; a blend of LDPE and EVA (ethylene vinyl acetate copolymer with a reported VA content of 14%), i.e., NEE foam; and a blend of EVA and EPR (ethylene propylene rubber with a proportion of 28% propylene), i.e., NSR foam.

Two kinds of foams can be distinguished: ALVEOLIT ("T" samples) are closed-cell, phys-

ically crosslinked polyolefin foam sheets. In this foaming method the sheet is crosslinked by a high energy electron beam, before the foaming agent is heat activated. Foaming direction is vertical; this means the foamable sheet passes from top to bottom through a hot oven (air /IR heated).

ALVEOLEN ("N" samples) are fabricated in a similar manner, although the foaming process is carried out in a horizontal plane. This means the foamable sheet passes horizontally through a hot air-heated foaming oven. The expanding sheet is carried out on a belt and supported by an air layer.

EXPERIMENTAL

Microscopic Characterization

DSC (Differential Scanning Calorimetry)

Thermal properties were studied by means of a Mettler DSC30 differential scanning calorimeter, previously calibrated with indium. The weights of the foam samples were approximately 3.5 mg. The experiments were carried out between −40 and 200°C, with a heating rate of 10°C/min.

Two characteristic properties of the polymer that comprises the cell walls of the foams were obtained. The melting point (T_m) was taken as the minimum of the melt peak in the enthalpy curve. Some of the blends presented two melt peaks, each one associated with each polymer that makes up the blend. In this case, two melting points were obtained.

The crystallinity of the polyethylene foams was calculated from the DSC curve by dividing the measured heat of fusion by the heat of fusion of a 100% crystalline material (288 J/g).[5]

The determination of the heat of fusion from the area of the DSC peak can be performed after establishing a baseline to bind the area that is to be integrated. In this work, the derivative curve is used to calculate the onset temperature,[6] the departure of the thermal curve from a horizontal baseline.

SEM (Scanning Electron Microscopy)

Quantitative image analysis was used to asses type of cellular structure and mean cell size. For this purpose, cross-sections of extrudate were microtomed at low temperature to provide a smooth surface, which, after vacuum coating with gold, was examined by SEM using a JEOL JSM 820. Each micrograph was analyzed by obtaining data from 10 reference lines. Apparent mean cell size was estimated by calculating the number of cells that intersected each reference line, and dividing the appropriate reference length by the number of cells.[7]

Usually foams present anisotropic properties due to their cell shape and, in general, the cells have a higher size in the parallel direction to the foaming direction[8] (cells are elongated in the foaming direction). Therefore, it is necessary to measure the cell size in the three principal directions (machine direction, crossdirection and thickness direction).

Macroscopic Characterization

Density Measurements

Foams samples were conditioned at 24°C and 50% relative humidity for 24 h and subjected to density measurements in accordance with ASTM D1622.

Compression Experiments at Low Strain Rates

Stress (σ) strain (ϵ) curves were measured with an Instron machine (model 5500R6025) at room temperature and at a strain rate of $d\varepsilon/dt = 10^{-1}$ s^{-1}. The maximum static strain was approximately 75% for all the experiments.

After this first load program, the stress–strain recovery behavior at a rate of -10^{-1} s^{-1} was also measured. This load and recovery program was applied five times to the samples (five consecutive cycles). The five cycles were used to study the influence of the mechanical history on the properties of each foam. The diameter of the samples was 10 cm, and the thickness is shown in Table I. The materials were tested as received (variable thickness, depending of the foam) to be able to compare the results of the compression experiments with those of the impact tests. Each type of material was tested three times to obtain the average response.

Two mechanical properties were obtained from these experiments. (1) The slope of the initial zone of the stress strain curve for each cycle, E^i. For the first cycle, this slope can be considered as the elastic modulus of the material, E^1. (2) The unrecovered strain for each cycle nr^i ($i > 1$, $nr^1 = 0$) (plastic strain).

$$nr^i\ (\%) = \frac{\varepsilon_0^i}{\varepsilon_m^{(i-1)}}\,100 \qquad (1)$$

where $\varepsilon_m^{(i-1)}$ is the maximum strain in the cycle number $(i-1)$, and ε_0^i is the minimum strain in the cycle number i.

Instrumented Falling-Weight Impact Tests

Instrumented falling-weight impact tests were carried out using a DARTVIS (CEAST, Torino) instrumented impact equipment. The dart had a hemispherical headstock of a 12.7 mm diameter, instrumented by extensometric gauges, that allows one to obtain force/time curves.

Foams were received as plaques of 300 × 200 mm and variable thickness, depending on the type of foam (Table I). From these plaques, disks of 80 mm diameter were cut off, to use them as impact test specimens. These were fixed on both sides (clamping system) by means of rings of inner and outer diameter of 60 and 80 mm, respectively.

Two types of tests were performed both at room temperature.

First, failure tests using a dart mass (m) of 3743 g and a drop height of 990 mm were performed. At these conditions the dart penetrated fully the foams, and the dynamic effects and the percentage of energy lost by the dart were negligible in all cases. Then, the static analysis[9] can be applied (Fig. 1) to obtain the foam failure strength as the maximum tensile stress value[10]

$$\sigma_{\max} = \frac{F_{\max}}{h^2}(1+\nu)\left(0.485 \log \frac{a}{h} + 0.52\right) \quad (2)$$

where $F_{\max}$ is the maximum force, h is the sample thickness, a is the specimen radius, and ν the Poisson's ratio of the material (we have used a value of $\nu = 0.04$ for all the foams).[11]

We also determined a foam toughness value defined as the energy lost by the falling dart until when the maximum force was reached, divided by the main sample volume involved in the failure (dart headstock transversal area multiplied by the sample thickness).

Second, to determine values of the elastic modulus, low-energy rebound tests were carried out employing a dart mass of 743 g, and a selected fall height range for each foam. A minimum of 10 different rebound heights were tested per foam. From the recorded force/time curves, the values of the maximum force ($F_{\max}$) and the contact time (t_c) were taken, and two values of the elastic modulus were calculated (E_{fmax} and E_{tc})[12]

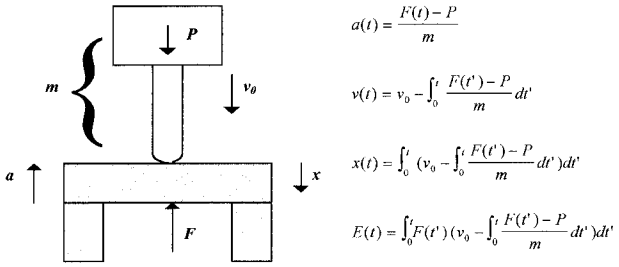

Figure 1 Geometry and equations of the static analysis for falling-weight tests.

$$E = \frac{3(1-\nu^2)a^2K}{4\pi h^3}$$

$$K = \frac{1}{m}\frac{F_{\max}^2}{v_0^2} \text{ or } K = \frac{m\pi^2}{t_c^2} \quad (3)$$

where K is the rigidity and v_0 is the initial speed.

The average value of E_{fmax} and E_{tc} was considered as a representative value of the elastic modulus of each foam (E^{reb}).

Dynamic Mechanical Analysis

The storage modulus (E'), loss modulus (E''), and loss tangent (tan δ) were obtained in a parallel-plate measurement system, a configuration suited for the porous nature of the samples. These properties were measured at 1 Hz in the temperature range between −40 and 100°C, with a heating rate of 5°C /min. The applied static strain and dynamic strain were chosen in the low strain range (2% static strain and 0.1% dynamic strain), where the mechanism that controls the sample's behavior is the cell walls bending.[8] The plate diameter was 10 mm, and the test specimens were prepared in a cylindrical shape with the same diameter.

RESULTS

Differential Scanning Calorimetry (DSC)

The thermal properties of the foams are presented in Table II. There are not significant differences between foams of the same type (same chemical composition and density).

Some of the blends (LDPE/HDPE and LDPE/EVA) showed two meting peaks (Table II). However, the two peaks were not completely separate for the other blends (LDPE/LLDPE and EVA/

Table II Thermal Properties of the Foams

Sample	Heat of Fusion (J/g)	Melting Temperature (°C) (First Peak)	Melting Temperature (°C) (Second Peak)	Crystallinity (%)
NLB1106	119.4	107.8	—	41.5
NLB1408	113.4	106.1	—	39.4
NLB2910	107.7	107.4	—	37.4
NA1106	113.7	109.1	—	39.5
NA2006	116.5	108.6	—	40.5
NA3308	116.7	109.1	—	40.5
NEE1109	89.1	88.3	107.7	—
NSR2512	61.4	86.9	—	—
NT0905	146.3	105.6	125.3	50.8
NT2510	136.5	106.1	126.3	47.4
TL2005	112.3	105.2	—	39.0
TL3008	100.9	104.2	—	35.0
TA1504	120.9	104.7	—	42.0

EPR). Consequently, for these materials, only one peak was determined (Table II).

The morphology of the crystalline phase of the polyethylene foams is different, depending of the kind of polyethylene. This result can be inferred from the shape of the melting peaks and from the crystallinity data.

NT foams with a 40% HDPE content have a higher crystallinity than the foams made of 100% LDPE (NA and TA foams) or blends of LLDPE and LDPE (NLB and TL foams).

Alveolen materials made of 100% LDPE (NA) or based on blends of LDPE and LLDPE (NLB) have approximately the same crystallinity; however, the morphology of their crystalline phases is different, which can be deduced from the different shape of their melting peaks (Fig. 2). The same result can be observed for the Alveolit materials made of 100% LDPE (TA) or based on blends of 50% LDPE, 50% LLDPE (TL) (Fig. 2).

Moreover, although there are not significant differences between the crystallinities of TA and NA foams with the same chemical composition, their crystalline structures are also slightly different, which can be inferred from their different melting points (slightly higher for the N foams).

Scanning Electron Microscopy (SEM)

Two typical images of the cellular structure of the foams under study are shown in Figure 3. In these micrographs the sections of one Alveolit [(a) TL2005)]and one Alveolen foam [(b) NA2006] of similar densities cut parallel to the foaming direction (machine direction, which is perpendicular to the measurement direction) can be observed.

The data for the cell size in the machine, cross, and thickness directions are presented in Table III. Both kinds of foams have anisotropic cells, with a larger cell size in the parallel direction to the foaming direction. The degree of anisotropy can be characterized by means of the ratio between the larger cell size and the smaller cell size.[13] In general terms, it can be said that Alveolen foams have larger cells and lower anisotropy ratio than Alveolit foams. The materials have anisotropic cells due to the foaming process. In

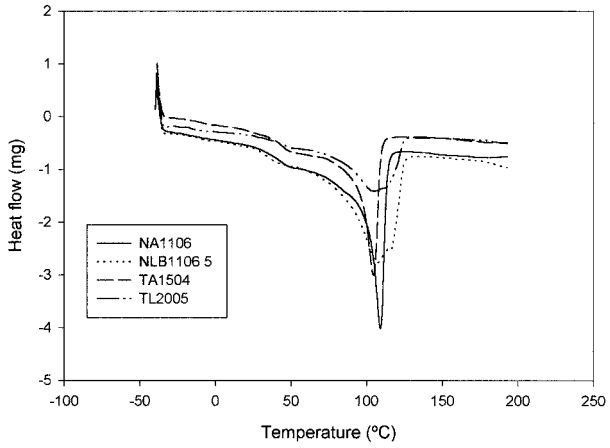

Figure 2 Thermograms of some of the foams under study: NA1106, NLB1106, TL2005, TA1504.

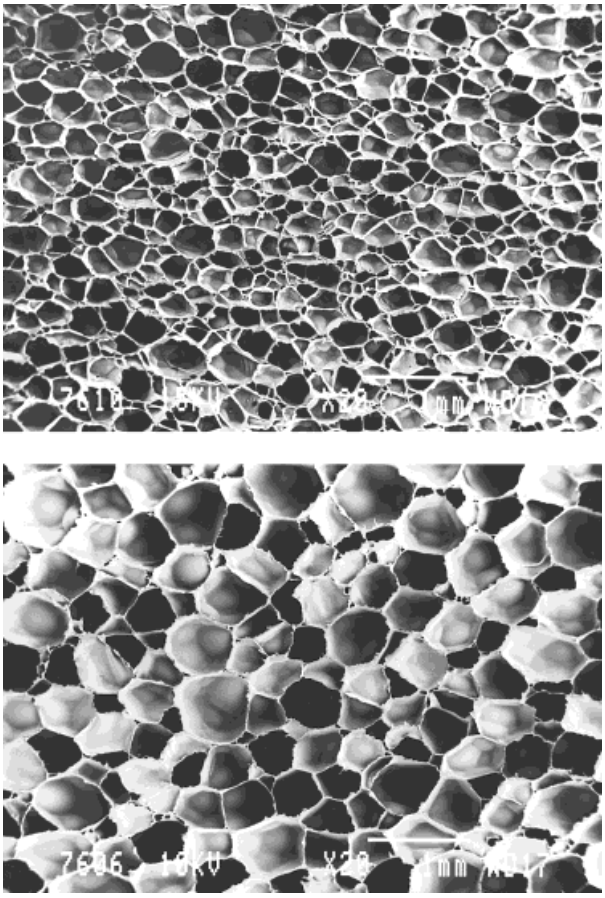

Figure 3 Micrographs of two typical materials: (a) Alveolit foam (TL2005), (b) Alveolen foam (NA2006).

these foaming methods the sheet is stretched during the expansion, which results in elongated cells in the machine direction. The stretching is higher for the Alveolit foams resulting in more elongated cells.

Compression Experiments

Figure 4 shows a typical example (NA3308 foam) of the two mechanical properties obtained from the compression experiments as a function of the number of cycle.

It can be concluded that the behavior of the materials is very different after the first cycle. This is due to the plastic deformations in the cell walls that occur during the first cycle, in which the strain reached a value of 75%. As a consequence of the previous result, it is evident that it is very important to study the properties as a function of the cycles. Usually, only the data for the first cycle are recorded, although, for these materials, this value cannot be used to design parts for applications where the material is subjected to repeated loading.

The slope of the initial part of the stress–strain curve in the first and fifth cycles, and the unrecovered strain as a function of the density can be observed in Figure 5. Both physical properties increase when the density of the foamed material increases.

The result for the elastic modulus is well known.[1,8] E^1 can be theoretically described as a potential law of the density (ρ), $E^1 = A\rho^n$, with $n = 2$ for open cell foams and $n = 1$ for closed-cell foams with a uniform distribution of the solid in the cell faces and edges.[14]

On the other hand, it is also well know that the driving forces for the recovery of closed-cell foams

Table III Basic Characteristics of the Cellular Structure of Each Foam

Sample	Cell Size in the Machine Direction (μm)	Cell Size in the Crossdirection (μm)	Cell Size in the Thickness Direction (μm)	Anisotropy Ratio
NLB1106	248	205	190	1.31
NLB1408	249	240	239	1.04
NLB2910	282	275	262	1.08
NA1106	278	260	236	1.18
NA2006	315	283	261	1.21
NA3308	438	402	376	1.16
NEE1109	258	225	220	1.17
NSR2512	341	330	311	1.10
NT0905	249	210	192	1.30
NT2510	352	330	320	1.10
TL2005	193	175	152	1.27
TL3008	200	182	170	1.18
TA1504	193	173	153	1.26

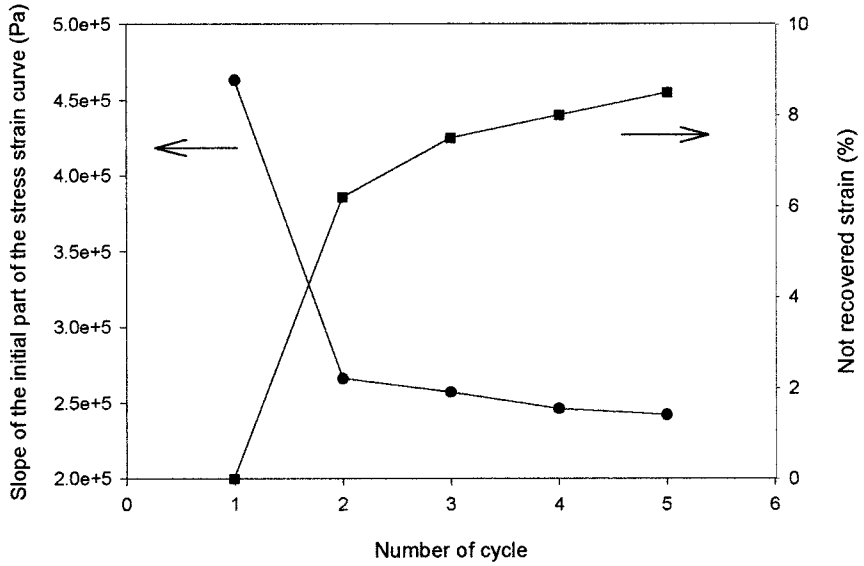

Figure 4 Compression properties for the NA3308 foam as a function of the number of cycle. (a) Slope of the initial zone of the stress strain curve. (b) Unrecovered strain.

could be the related to the compressed gas inside the cells or to the viscoelastic recovery of the cell walls.[4,15] The experimental results show that for the kind of experiments carried out (recovery from 75% static strain at a constant strain rate of 10^{-1} s^{-1}) the foams with lower density (higher gas content) have a better recovery, which seems to indicate that the compressed gas inside the cells plays an important role in the recovery behavior of these samples.

The trends observed as a function of the chemical composition for foams with similar density, and for the same kind of foaming process, were similar to those expected for continuous (noncellular) solid polymers. For the Alveolen foams the results were:

elastic modulus (E^1): NT > NL ≈ NA > NEE or NSR

unrecovered strain (nr^5): NT > NL ≈ NA > NEE or NSR

(Note: it is not possible to directly compare the properties of the NSR and NEE foams because they have different densities. However, from the experimental results it is clear that the elastic modulus and unrecovered strain of these materials are lower than that of the NA foam.)

Moreover, these two mechanical characteristics also depend on the kind of foaming process. Figure 5 shows that both elastic modulus and unrecovered strain are higher for the Alveolen (N) foams. Two contributions have to be taken into account to explain these results. First, Alveolen foams present more isotropic cells with a larger diameter, which results in a higher strain resistance. Second, these materials have a different morphology of the crystalline structure than the Alveolit (T) foams of the same chemical composition (DSC results).

Impact Experiments

The mechanical characteristics that were obtained from the instrumented falling-weight tests are presented in Figure 6. The main results are summarized as follows: (a) as expected, the failure strength, toughness, and elastic modulus increased with the foam density. (b) T foams show higher failure strength and stiffness than N foams of similar density and chemical composition, although the toughness of both kinds of samples was found to be almost equal. The geometry imposed in these tests is flexion, which causes tensile stresses on the specimen during the dart contact. Therefore, T foams, which have more elongated cells in the direction of the tensile stresses, presented higher values of strength and elastic modulus than N foams. (c) The comparison between foams of different chemical composition and similar density gives, for the Alveolen (N)

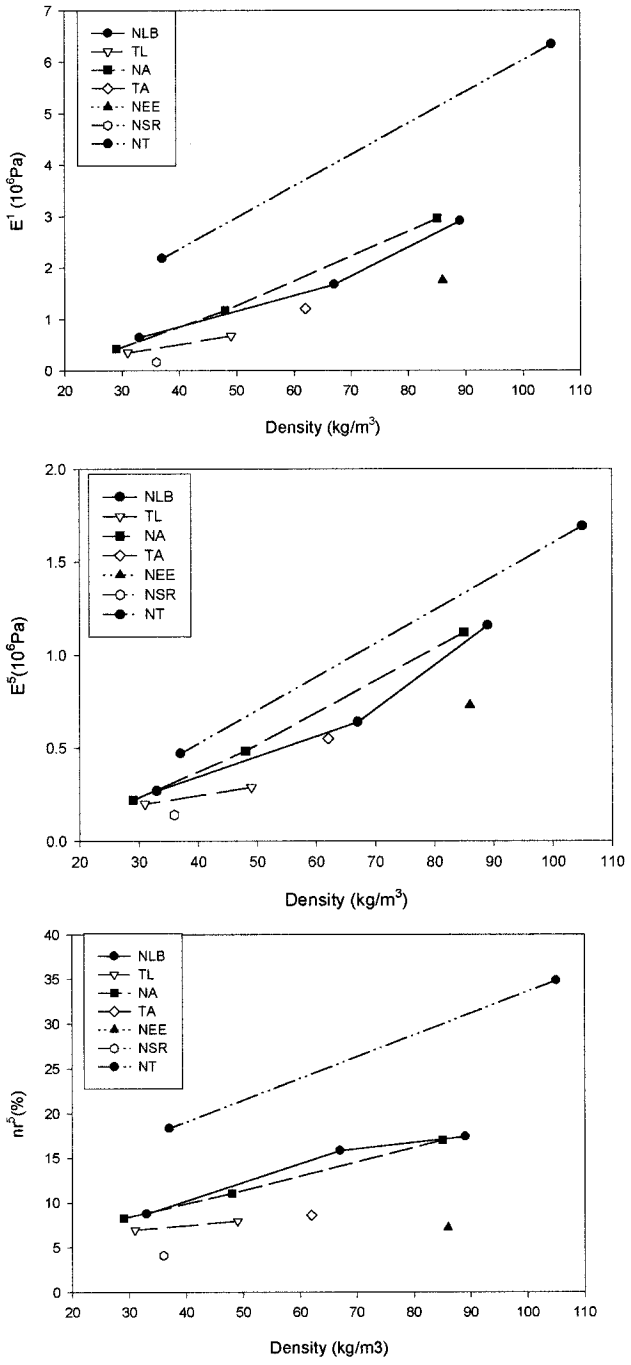

Figure 5 Compression properties as a function of the density. (a) E^1, (b) E^5, (c) nr^5.

samples with higher densities, the following trends:

failure strength: NT > NL ≈ NA > NEE or NSR

toughness: NSR or NEE > NL > NT > NA

elastic modulus: NT > NL ≈ NA > NEE or NSR.

It can be observed that the elastic modulus trend is the same as we have found by compres-

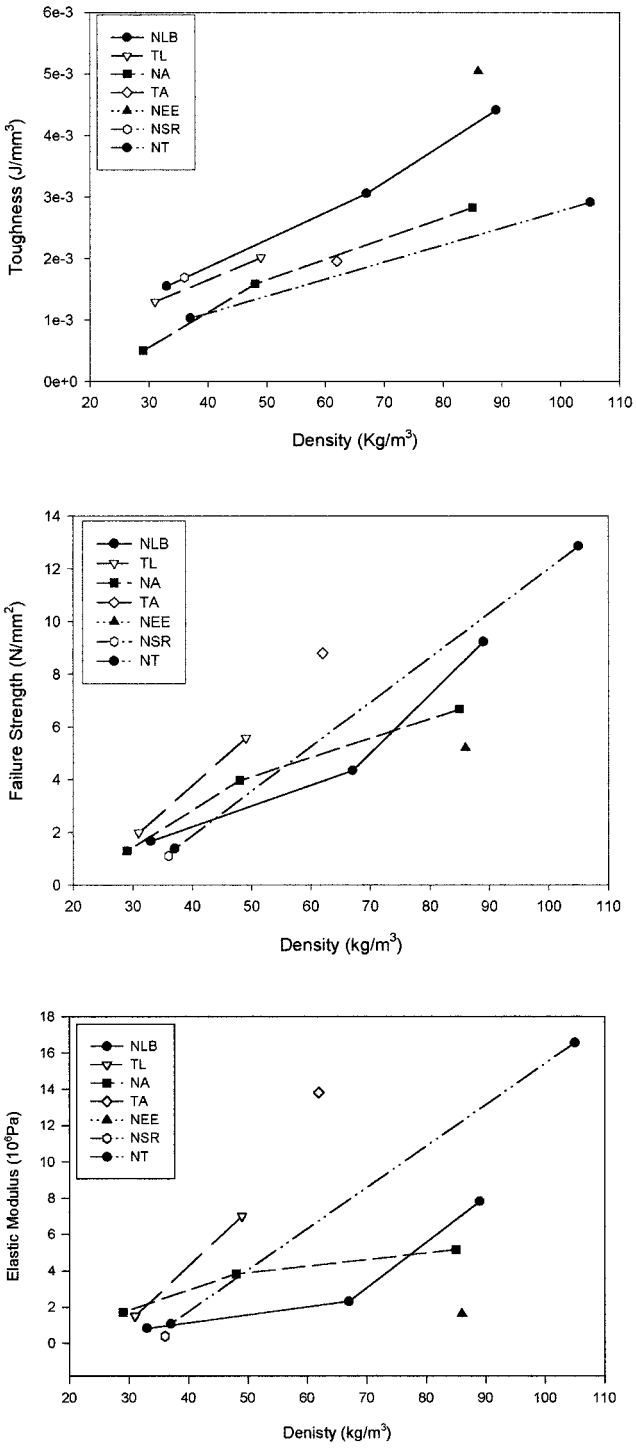

Figure 6 Falling-weight impact tests: (a) toughness, (b) failure strength, (c) elastic modulus.

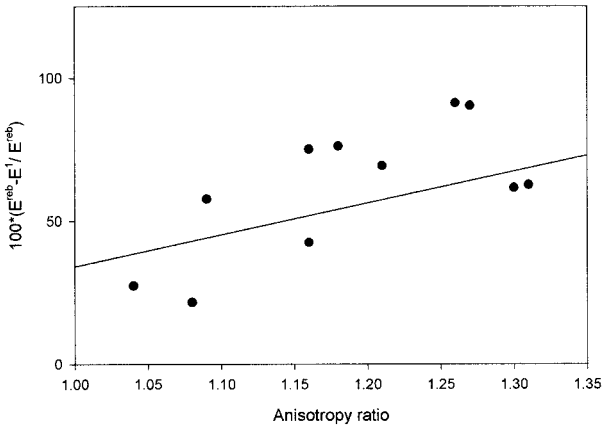

Figure 7 Difference between the Young modulus obtained in the compression experiments and that obtained in the impact tests as a function of the anisotropy ratio.

sion. Because of the rubbery nature of the EVA (present in the NEE and NSR foams), they showed higher values of toughness, whereas the more rigid (NT) foams showed the lowest. Nevertheless, the elastic modulus obtained from the rebound tests was higher than those obtained from the compression test. On one hand, the higher strain rate imposed in the rebound tests makes these polymeric samples more rigid due to their viscoelastic character, and, on the other hand, as pointed before the tensile stresses produced on the samples by the flexural geometry applied in the rebound experiments also contribute to increase the values of the elastic modulus. These differences are related to the anisotropy ratio of each foam in Figure 7. In general terms, it can be concluded that the difference is higher for the more anisotropic foams. (d) We have observed that these foamed samples, because of their softness, suffered an important indentation effect when they were subjected to the rebound tests. This contribution was not taken into account in the determination of the elastic modulus by rebound (E^{reb}), because the applied equations are just a model for linear-elastic flexed plates. Then, although the trends were the same as obtained in pure compression testing, the measured value may not be absolute.

Dynamic Mechanical Properties

The dynamic mechanical experiments were carried out in the low strain range, where the main contribution to the foam viscoelasticity is given by the solid polymer.[16] To rationalize the experimental results, it is necessary to take into account that nonmiscible polymer blends have a viscoelastic response intermediate between the two polymers that made up the blend.

A typical example of the viscoelastic response of foams with different chemical compositions is shown in Figure 8 (the qualitative behavior was the same for foams with the same chemical composition and kind of foaming process). The well-known viscoelastic relaxations for each type of polymer can be observed. The PE foams present the typical behavior of nonfoamed polyethylene. At low temperatures (approximately −20°C) the β relaxation can be detected as a peak in the loss modulus curve or as a shoulder in the tan δ curve. This relaxation results from motions of chain units located in the interfacial region, and its

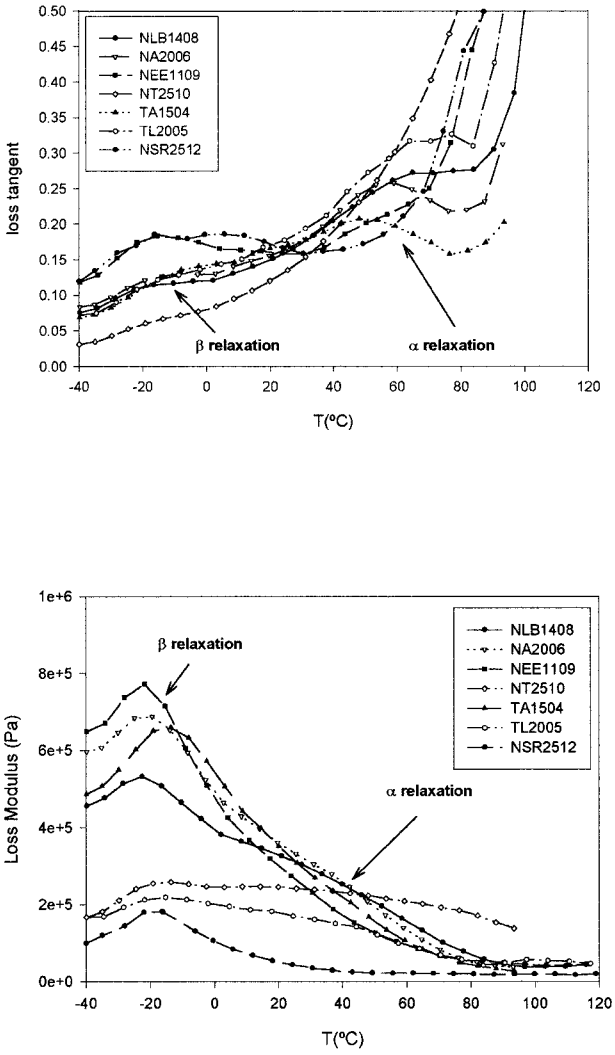

Figure 8 Typical dynamic mechanical response of different materials (a) loss tangent, (b) loss modulus.

existence is not universal in different types of polyethylenes, being controlled by the presence of an interfacial content higher than about 7%.[17] Because of this, the relaxation has been clearly detected in branched polyethylene (LDPE), and has not been detected at all in linear polyethylene of medium molecular weight, by using dynamic mechanical methods.

This relaxation is present in all the materials under study, because all of them have a high LDPE content. While the NL, TL, NA, and TA foams have a similar relaxation, the intensity of this relaxation is higher for the NEE and NSR foams, which is associated with a higher interfacial content in the EVA copolymers. This intensity is lower for the NT foams due to the lower interfacial content of the HDPE phase.

The α relaxation can be seen at higher temperatures (approximately 50°C) as a wide peak in the tan δ curve or as a shoulder in the E'' curve. The relaxation can be associated with the crystalline part of the polymer. The intensity of this relaxation increases when the crystalline content increases and the position is controlled by the lamella thickness, the peak is shifted to higher temperatures for materials with higher lamella thickness.[18]

Taking into account the previous results for nonfoamed polyethylene, it is possible to infer some conclusions from the DMA experiments. The relaxation is not visible for the NSR and NEE foams, which is due to their low crystalline content. The position of peak is different depending of the kind of foam. NL foams have their peak at higher temperatures than NA foams, which it is related with the different crystalline structure of these two types of materials. NL foams seems to have thicker lamellae. The peak is not clearly observed for the NT foams in the tan δ curve, but it appears as a strong peak in the loss modulus curve, which can be explained in terms of the higher crystallinity of these materials.

Also, it is possible to observe some differences between the viscoelastic response of the T and N foams. The TA foams have the peak at lower temperatures than the NA foams, which agrees with the thermal results that indicate a different morphology of the crystalline structure for these two types of foams.

On the other hand, the storage modulus and loss tangent of the foams at room temperature has been plotted in Figure 9. It can be observed that the storage modulus increases when the density increases, and that the loss tangent slightly decreases when the density increases.

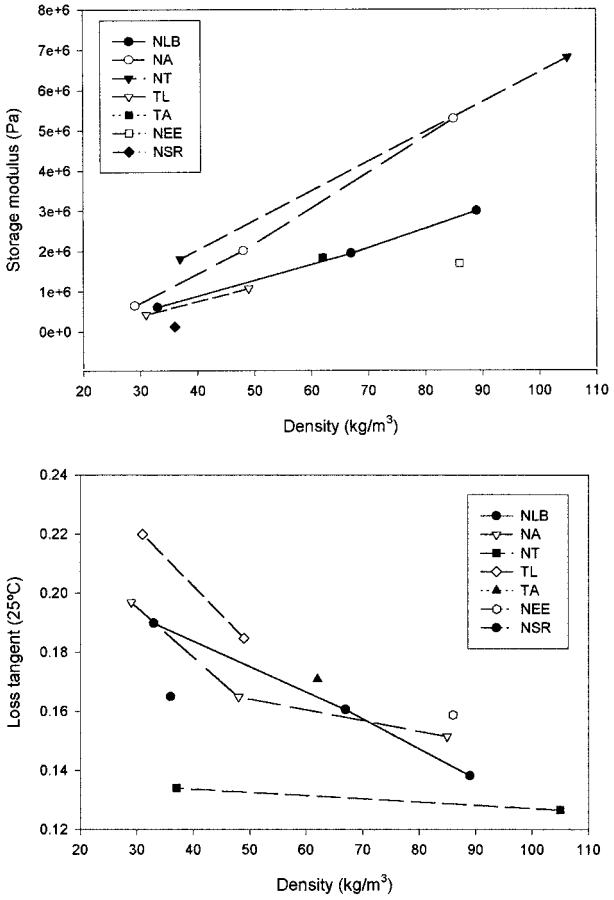

Figure 9 DMA results at room temperature (25°C) as a function of the density: (a) storage modulus, (b) loss tangent.

The results as a function of the chemical composition for the Alveolen foams are as follows:

storage modulus (E'): NT > NA > NL > NEE or NSR

loss tangent (tan δ): NA $\approx$ NL $\approx$ NEE or NSR > NT.

From this technique it is also possible to identify some differences between the storage modulus and loss tangent of T and N materials. T materials have a slightly higher loss tangent and a lower storage modulus.

Finally, it is interesting to point out the difference between the storage modulus of the NA and NL foams (Fig. 9), which it is not possible to observe in the elastic modulus obtained by compression and rebound tests.

CONCLUSIONS

Three different experimental techniques have been used for the mechanical characterization of a collection of crosslinked closed-cell polyolefin foams.

From the low-rate compression experiments, it can be pointed out that the mechanical behavior of these materials depends on the number of cycle. This result has to be taken into account in real applications.

From the impact experiments, the failure strength, the toughness, and the elastic modulus at high strain rates were obtained. In general, the foams showed elastic modulus higher than that obtained from the compression experiments, which is due first, to the higher strain rate, and second, to the different mode of deformation. It should be necessary to take into account the indentation contribution to obtain more accurate results for the elastic modulus values.

From the dynamic mechanical experiments, it was possible to measure the storage modulus and loss tangent as a function of the temperature, and the intensity and temperature of the foams relaxations. From these data, conclusions about the structure of the base polymer can be obtained. Different foam compositions promote different crystalline structures, which affect their mechanical response.

On the other hand, some relationships between the structure and properties of the foams have been shown. Some of the most important are: (a) the different mechanical properties of foams made of different types of polyethylene can be explained in terms of the different crystalline structure of these materials. (b) All the materials under study have an anisotropic cellular structure. The cells are elongated in the foaming direction and, in general terms, the degree of anisotropy is higher for the Alveloit foams than for the Alveolen foams. This is one of the main reasons for the differences found between the elastic modulus obtained by rebound and by compression tests. (c) The elastic modulus and the storage modulus increased with the foam density. The unrecovered strain also increased with the density, which seems to indicate that the gas compression plays an important role in the recovery of these foams. (d) The trends observed as a function of the chemical composition, for almost all the properties under study, are similar to those of continuous noncellular solids. (e) The elastic modulus, unrecovered strain, failure strength, storage modulus, and loss factor depend on the type of foaming process. This is mainly due to two contributions, the cell shape and/or the crystalline morphology of the base polymer.

Financial assistance (O. Almanza) from COLCIENCIAS (Colombia) is gratefully acknowledged. We also thank Sekisui Alveo BV for supplying the foams.

REFERENCES

1. Hilyard, N. C.; Cunningham, A. Low Density Cellular Plastics: Physical Basis of Behaviour; Chapman and Hall: London, 1994.
2. Corsaro, R. D.; Sperling, L. H. Sound and Vibration Damping with Polymers; American Chemical Society: Washington, DC, 1990.
3. Loveridge, P.; Mills, N. J. Cell Polym 1991, 10, 393.
4. Mills, N. J.; Hawng, A. M. H. Cell Polym 1989, 9, 259.
5. Wunderlich, B. In Macromolecular Physics; Academic Press: New York, 1973–1976, vol. 2.
6. Castelli, R.; Deplano, M.; Rota, P. M. J Thermal Anal 1996, 47, 117.
7. Sims, G. L. A.; Khumiteekoll, C. Cell Polym 1994, 13, 137.
8. Gibson, L. J.; Ahsby, M. F. Cellular Solids: Structure and Properties; Pergamon Press: Oxford, 1988.
9. Casiraghi, T.; Casfiglioni, G.; Ronchetti, T. J Mater Sci 1988, 23, 459.
10. Timshenko, S. P.; Woinwsky-Krieger, S. Theory of Plates and Shells; McGraw-Hill: Tokyo, Japan, 1984.
11. Wilsea, M.; Johnson, L. K.; Ahsby, M. F. Int J Mech Sci 1975, 457.
12. Martinez, A. B.; Arnaw, J.; Santana, O.; Gordillo, A. Inform Tecnol 1994, 5, 19.
13. Cowin, S. C. J Mater Sci 1991, 26, 5155.
14. Weaire, D.; Fortes, M. A. Adv Phys 1994, 43, 685.
15. Rodríguez-Pérez, M. A.; Díez-Gutiérrez, S.; de Saja, J. A. Polym Eng Sci 1998, 38, 831.
16. Rodríguez-Pérez, M. A.; Rodríguez-Llorente, S.; de Saja, J. A. Polym Eng Sci 1997, 37, 959.
17. Popli, R.; Glotin, M.; Manderlkern, L.; Berson, R. S. J Polym Sci Polym Phys Ed 1984, 22, 407.
18. Alberola, N.; Cavaille, J. Y.; Pérez, J. J Polym Sci Polym Phys Ed 1990, 28, 569.